# Performance Evaluation of Drone Operated Dual Waveform Bathymetric LiDAR

Joonas Kousa <sup>1</sup>, Teemu Hakala <sup>2</sup>, Antero Kukko <sup>2</sup>, Harri Kaartinen <sup>2</sup>

<sup>1</sup> Aalto University, 02150 Espoo, Finland – joonas.kousa@aalto.fi

<sup>2</sup> Dept. of Remote Sensing and Photogrammetry, Finnish Geospatial Research Institute FGI at the National Land Survey of Finland, 02150 Espoo - teemu.hakala@nls.fi, antero.kukko@nls.fi, harri.kaartinen@nls.fi

**Keywords:** Bathymetry, Laser scanning, Multispectral, Drone, Performance, LiDAR.

#### Abstract

Flooding has been the most critical environmental threat to human settlements already for decades and due to climate change both the quantity and the volume of floods are increasing globally, making surveying and studying of water environments an ever-increasing interest. Drone-based surveying technologies are an effective method for detailed surveying of topography, and recently systems for bathymetric measurement have emerged. Fraunhofer Airborne Bathymetric Laser Scanner (ABS) is the first truly lightweight drone operated sensor for simultaneous multiwavelength topographic and bathymetric data acquisition for seamless water environment mapping. To assess the precision, spatial resolution, depth performance and bathymetric accuracy of the novel ABS system, tests were carried out both in dry land and water environment in varying weather conditions. Assessments of the precision and spatial resolution from topographic targets provide standard deviation of approximately 1.5 cm and spatial resolution of 2.5 cm. Despite inconsistencies on targets with low reflectance, the results confirm that the topographic performance is comparable to similar devices and suitable for operation. The bathymetric capabilities of the sensor exceed expectations providing depth penetration of 1.75 Secchi depths in ideal conditions and 1.25 Secchi depths in challenging conditions from all tested flight altitudes. The experimental results demonstrate that the topographic and bathymetric performance of the ABS fulfil the specifications presented by the manufacturer and confirm that the device is suitable to be used for mapping water environments using UAV platform.

#### 1. Introduction

Bathymetric LiDAR is a remote sensing method utilizing water penetrating pulsed laser to gain accurate measurements of underwater topography. Detailed 3D point clouds can be created from such LiDAR measurements, with precise position and orientation data. Bathymetric LiDAR sensors and airborne laser bathymetry (ALB) have been shown to be viable methods in shallow-water mapping already for decades, but traditionally the systems have required a full-size/crewed aircraft for operation (Guenther et al., 2000). With the further development of LiDAR sensors, their size has decreased and bathymetric LiDAR systems based on UAV (Unmanned Aircraft Vehicle) have been introduced, allowing more agile and cost-effective data collection and more precise data (Mandlburger et al., 2020; Islam et al., 2021). As UAV-based systems are flown at lower altitudes, the laser beam divergence does not increase the laser footprint nearly as much as in larger sensors operated using manned aircraft (Fernandez-Diaz et al., 2014; Okhrimenko and Hopkinson, 2019; Wang et al., 2022), resulting in better precision in both topographic and bathymetric measurements. However, most of these smaller LiDAR sensors operate only with a single wavelength, thus lacking the possibilities provided by multiwavelength laser scanning.

The multiwavelength capability is substantial for the potential applications of ALB (Pfennigbauer and Ullrich, 2011; Vosselman and Maas, 2010), not only for determining the level of water surface, but also to gain better topographic and texture data as the fluvial environment does not end to the water's edge. Instead the whole system is important, since sediments and vegetation on the catchment area have an extensive impact shaping the waterways (Young and Ashford, 2006). Therefore, multiwavelength ALB enables accurate modelling of shallow water environments such as rivers, lakes and coastal areas, which is necessary for numerous tasks in the field of hydrology,

hydrobiology, hydromorphology and hydraulics, such as flood simulation, erosion modelling, sediment type identification, and habitat mapping (Alho et al., 2009; Kasvi et al., 2019). Flooding has been the most critical environmental threat in Europe for decades and due to climate change both the quantity and volume of floods are increasing globally. This makes bathymetric surveying and study of aforementioned water environments and adjacent settlements an ever important undertaking (Hirabayashi et al., 2013).

Long-term repetitive data acquisition is essential to model the evolution of natural entities and thus also to predict any possible changes and environmental risks (Heino et al., 2020), further emphasising the need for UAV based systems. Currently, only a few multiwavelength bathymetric LiDAR sensors are available, and most of them need to be operated with manned helicopters or airplanes. The Airborne Bathymetric Laser Scanner (ABS) from Fraunhofer Institute for Physical Measurement Techniques (Fraunhofer IPM) is a lightweight multiwavelength LiDAR sensor that simultaneously emits both green ( $\lambda = 515$  nm) and near-infrared (NIR,  $\lambda = 1030$ nm) laser pulses (Fraunhofer IPM a and b). Additionally, the device makes use of the same optics for both wavelengths to minimize inaccuracies caused by differing measurement geometry usually present in multi-sensor applications. The weight of the system is approximately 4 kg so it can be fairly easily mounted on UAVs.

In this article the performance of the ABS is evaluated in order to determine its suitability for surveying shallow-water environments. The main contribution of this paper is to produce an unaffiliated evaluation of the performance of the novel LiDAR sensor as well as to verify its suitability for freshwater mapping. The paper is organized as follows. In Section 2 the ABS is presented and study areas and methods are described in more detail. Obtained results are presented in Section 3 and

further discussed in Section 4. Lastly, Section 5 concludes the key findings of the paper.

### 2. Material and Methods

### 2.1 The Airborne Bathymetric Laser Scanner

The Fraunhofer ABS is a compact multi-wavelength topobathymetric LiDAR scanner designed for surveying shallow water bed topography. Its novelty value is based especially on two features: light weight and coincident optical paths of the two wavelengths. The scanner unit weighs 3.3 kg and the integrated system as a whole approximately 4 kg allowing multi-wavelength ALB using UAVs, particularly commercially available drones. According to Fraunhofer IPM, different versions of the sensor are also available, with gross weights starting at only 2.5 kg. The identical optical path for the both wavelengths is achieved by separating the wavelengths with a dichroic mirror only in front of the detector chips (Fraunhofer a; Werner et al., 2023). This essentially eliminates errors caused by differences in optics or the relative positioning of laser sources. The device is shown in Figure 1.



Figure 1. The ABS on its side on top of the transport box. The rotating mirror is visible through the round window.

The size of the ABS is 310 mm  $\times$  180 mm  $\times$  100 mm and it can be mounted on UAVs utilizing mounting screw holes on the backside of the device. The ABS is powered by an external source; additional battery, or alternatively using a power outlet from the UAV. The scanner has a high speed solid-state drive (SSD) with capacity of 1 TB that is used to store the recorded data as well as to make pre-processing possible. The central processing unit of the ABS is capable of pre-processing data at rate of 50 Gb/s allowing more efficient data storage and transmission (Fraunhofer IPM a and b).

The announced penetration depth of the ABS is one Secchi, which is roughly a half of that of general large airplane-operated scanners. The Secchi depth (SD) corresponds the depth at which a Secchi disk is no longer visible to the human eye when lowered in the water (Idris et al., 2022). It provides a simple reference point for comparably quantifying LiDAR penetration depth.

The scanner uses Time-of-flight (ToF) method for range determination and is capable of recording full waveform of the backscattered pulse. The laser beams are emitted at an angle of 15° off-nadir and, according to the manufacturer, the diameter of the laser footprint at exit is approximately 50 mm, with divergence of 0.5 mrad for green wavelength and 2 mrad for NIR. The laser beam is expanded via a telescope designed to

collimate the beam (Werner et al., 2023). The scanner has an elliptical scanning pattern, which is implemented utilizing a rotating mirror with a 7.5° tilted surface rotating at the speed of 50 Hz (=3000 rpm) resulting in a conical scanning principle. The green channel uses wavelength of 515 nm, which is close but not exactly the same as the most commonly used 532 nm in LIDAR bathymetry. The NIR wavelength is 1030 nm and in bathymetric measurements it is primarily used to determine the level of water surface, allowing the calculation of refraction correction. This increases the accuracy of bathymetric measurements as underwater points can be correctly georeferenced (Westfeld et al., 2017). The announced pulse repetition frequency is 35 kHz. However, the frequency of the unit with serial number 2, used in the experiments described in this article, is 50 kHz. The pulse repetition frequency may likely be user adjustable in the future as the device and controls are still being developed.

Other features include for example a web interface to control the scanner and see its status as well as possibility for integrated Global navigation satellite system (GNSS) and Inertial measurement unit (IMU) so additional position and orientation modules would not be needed. The tested scanner unit does not have the integrated devices so an external NovAtel CTP7B GNSS-IMU system was used instead. The backside of the scanner has 1 Gb Ethernet port, a port for GNSS and IMU and power connector. The web interface is accessible either through Ethernet or Wireless Local Area Network (WLAN), the latter of which makes also wireless controlling and monitoring during operation possible as long as the sensor stays within the WLAN range. The light detector of the scanner uses photomultiplier tubes, in addition to linear mode avalanche photo diodes, to increase the sensitivity (Fraunhofer IPM a). Particularly the photon yield of green wavelength that has attenuated in the water body should benefit from this design. The laser of the scanner is classified as a class 2M according to EN 60825-1:2014 standard, which indicates that the emitted laser is safe for accidental (brief) viewing with naked eye, but may be hazardous if viewed with optical instruments (U.S. Marine Corps, 2014).

## 2.2 Study Areas

The study areas are located in Kirkkonummi in Southern Finland. The study area for bathymetry is in Lake Vitträsk (60°11'04.5"N 24°27'35.5"E), and for topography the study area is at Sjökulla test field (60°14'31.6"N 24°23'01.0"E). Lake Vitträsk has a surface area of 4.9 km² and maximum depth of 21.65 meters, being the largest lake in Kirkkonummi municipality. The lake is mostly surrounded by forest and sparse population. At the test site the dominating bottom sediments are sand and gravel.

Lake Vitträsk was selected as a study area since it is slightly turbid with a Secchi depth of approximately 2.4 meters, which is ideal as the water is clear enough to get data points from multiple depths but not crystal clear so it is a suitable example of a typical lake or river water in Finland. Also, noticeable differences between depths should exist at relatively shallow levels, which makes constructing reference targets easier.

The Sjökulla photogrammetric test field is a 0.4 ha area in northern Kirkkonummi, and its background is levelled with dark pebbles. Structures and artificial planar objects have been built into the area in order to test and calibrate topographic performance of LiDAR sensors. Additionally, the area has

rough grey level patterns for the purpose testing the resolution of aerial cameras, but those provide no useful information concerning LiDAR performance. The area is surrounded by agricultural fields, and climate type at the both study areas is warm-summer humid continental (Dfb) according to the Köppen climate classification system (Beck et al., 2018). Aerial photographs of both study areas are presented in Figure 2.

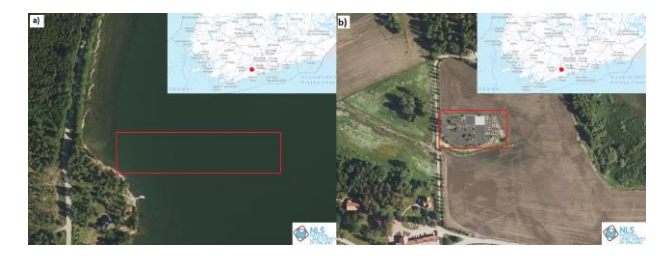


Figure 2. Aerial images of study areas.

### 2.3 Data Acquisition

To assess the performance of the ABS, two field campaigns were carried out on 12<sup>th</sup> and 22<sup>nd</sup> of September 2023 to gather the data. During these two days a total of eight flights were conducted: On the 12<sup>th</sup> three flights at Sjökulla from different altitudes and one at Lake Vitträsk, and on the 22<sup>nd</sup> four from different altitudes at Lake Vitträsk. During these experiments, the ABS was powered from external battery and paired with the previously mentioned NovAtel CTP7B-GNSS-IMU system for collection of position and orientation data. The system had two Harxon HX-CHX600A antennas with 1120 mm baseline to receive the signals from satellites and everything was attached to a carbon fiber chassis. The chassis with the whole laser scanning system was attached to a Walkera R1000 RTK drone. With this payload Walkera has approximately 20 minutes of flight time (Walkera, 2022).

On the  $12^{th}$  the weather was calm and partly cloudy with the temperature being approximately  $19^{\circ}\text{C}$  on both study areas. On the  $22^{nd}$  the weather was clearer, wind was stronger and temperature was about the same. At Sjökulla the flights were conducted by flying multiple straight lines across the test field at heights of 20, 50 and 100 meters. There were 1 m x 1 m Zenith Lite<sup>TM</sup> plates with differing reflectance (50%, 20%, 10% and 5%) on the ground providing an even/flat surface with a range of reflectivity. The plates are visible in Figure 3b.

On the 22<sup>nd</sup> flights at Lake Vitträsk matte light grey metal plates (size: 60 cm x 100 cm) were used as reference targets. The submerged metal plates are attached to Styrofoam floats from each corner by polyester rope. A total of four targets were used, one every meter from the depth of 2 meters to the depth of 5 meters (accuracy estimate ± 5 cm for each plate). Additionally, a Secchi depth measurement was carried out prior to the flights to determine accurate and comparable Secchi depth of the Lake Vitträsk study area at the time of data collection. The result of the Secchi depth measurement was approximately 2.4 meters. So the first plate was placed above Secchi depth and the rest below it. The plates were floated at steady depths corresponding to 0.8-2.1 SD. The manufacturer had announced the water penetration depth of the ABS to be 1 Secchi, thus the scanner should see the first plate clearly. Figure 3a shows the plates floating in Lake Vitträsk during the data acquisition on the 22<sup>nd</sup>. The picture has rather low resolution as it is captured from a live video feed transmitted from a webcam on-board the drone.

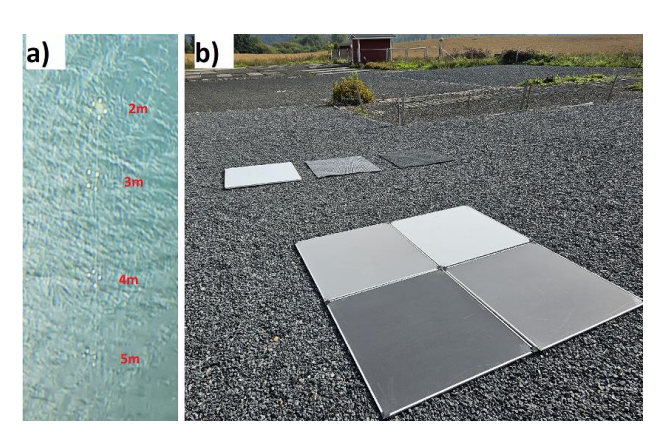


Figure 3. (a) Floating targets in Lake Vitträsk with depths annotated next to each plate. (b) Plates with different reflectivity values at Sjökulla test field.

At Lake Vitträsk one flight from altitude of 20 m was flown on the 12<sup>th</sup> and four flights from altitudes 20m, 35 m, 50 m and 80 m on the 22<sup>nd</sup> of October. The weather conditions were quite ideal on the 12<sup>th</sup> as it was cloudy, which reduces noise from sunlight, and quite calm, so the water surface was not choppy. On the 22<sup>nd</sup> on the other hand, the weather conditions were challenging as it was sunny, which exposes for increased noise, and windy, which caused quite large waves and choppiness. Therefore, it is expected that the scanner sees deeper on the 12<sup>th</sup> day's flight than on the 22<sup>nd</sup> day's flights. Each drone flight followed the same procedure: Initialization of the LiDAR sensor and the GNSS-IMU unit, take off and climb to mission altitude, data acquisition, descend and landing.

### 2.4 Data Processing

The laser scanner system collects raw full waveform data from the LiDAR unit and raw position and orientation logs from the GNSS-IMU unit. The flight trajectory was calculated from the position and orientation logs and GNSS base station data using Waypoint Inertial Explorer 8.90 software. The trajectory is exported from the software as a .pof file. It provides information of the LiDAR system's position and orientation at each moment of time, and the scanner is synchronised to the same time. The collected raw waveforms are then processed using Pulsalyzer software developed by Fraunhofer IPM specifically for the ABS. The software takes in the calculated trajectory and raw lidar data files. It extracts the full waveforms from the raw data and georeferences the extracted laser echoes, i.e. ranges, to geographic coordinates. In this way, the software constructs a 3D point cloud, which can then be exported as a .las or .laz file. The software is also able to do the refraction correction prior to exporting to correct the altered position of underwater points. This is done by first determining the level of water surface from the recorded points and then calculating the corrected position of points below that level with the software. The calculation to correct distorted underwater points is based on Snell's law and the refractive index of the air-water interface (Vosselman and Maas, 2010; Westfeld et al., 2017). The exported point clouds were opened in CloudCompare, which is a free to use open source software for inspecting point clouds (Girardeau-Montaut, 2015). The point clouds were cleaned with CloudCompare's SOR filter (Statistical Outlier Removal) using default settings to get rid of excess noise points. The filter calculates average distance to each point's k closest neighbours and then removes points, which are farther away than the average distance plus x times the standard deviation (default: k=6, x=1.0). The cleaned point clouds were then analysed and inspected using tools available in CloudCompare.

### 2.5 Evaluation Methods

The performance of the ABS was evaluated with four methods listed below. The methods used by Mandlburger et al. (2020) and Wang et al. (2022) are partly used in this paper.

- 1. Precision: The relative accuracy of the data points to assess the noise level of the sensor. This was studied by fitting a plane on the points of the smooth plates at Sjökulla test field and calculating the distance from each point to the plane. Standard deviation  $\sigma$  was also calculated. The plates used in the experiment are described more in detail in Section 2.3.
- Spatial resolution: The theoretical resolution determined by Fraunhofer IPM (Fraunhofer a and b; Werner et al., 2023) was compared to the resolution of collected point clouds by studying how objects can be detected from the data. The studied objects are various wooden edges between different types of pebbles at Sjökulla test field.
- 3. Depth performance: The maximum depth penetration of the sensor was quantified by comparing the deepest recorded data points to the measured Secchi depth. The light grey reference targets submerged to the lake were used to gain more standardized and comparable results. Additionally, the depth to which the lake bottom is visible was determined to gain a more situational insight.
- 4. Bathymetric accuracy: The recorded depth of data points from the detected reference targets was compared to the actual depth to which the reference targets were submerged in order to evaluate the reliability of depth profile obtained from the produced point clouds.

### 3. Results

### 3.1 Precision

The topographic precision is defined from measurements conducted at Sjökulla test field using reflectance plates, which are visible in Figure 3b. These values describe the ranging precision of the sensor and overall quality of the collected data. Due to having controlled test surfaces with multiple reflectance values, the effect of target's reflectance on precision can also be identified. The height difference between the lowest and highest point for all flight altitudes was approximately 7 cm, when the highest and lowest 0.5% of points are trimmed out of both ends of the recorded spectra. The results are trimmed to eliminate effect of random error. The standard deviation  $\sigma$  of the distribution is 1.53 cm and thus the height difference corresponds to 4.6 standard deviations.

The height difference of 7 cm is not an outstanding result in topography on modern standards, but it is a moderate result (Li et al., 2018; Elaksher et al., 2023) — especially when the intended usage of the LiDAR system is taken into account. Additionally, the height difference is affected by the deviating heights observed at the area of the darkest plate (the one with lowest reflectance), being approximately 2.5 cm lower than the mean of points in the area of all the other plates. This indicates that there could possibly be some calibration issues either in the

device or in the processing software, as there is no other clear reason for the observed height of the darkest plate to differ from others (Table 1). If this could be easily fixed, the height difference would likely decrease notably, since if only one plate (one reflectance) is looked at a time, the height difference in that homogeneous area is only approximately 3 to 5 cm depending on the plate reflectivity. Such performance already provides accurate and dense surfaces in the point cloud. Test flights were flown on three different altitudes but the altitude did not have a notable effect on the height difference or standard deviation. Furthermore, the inconsistency of the mean height for the darkest plate was present in the data from all altitudes. The flight altitude affected mainly on the point density, which also depends greatly on the flying speed.

Reflectance	Mean of height	Standard deviation σ	
5 %	6.581 m	2.55 cm	
10 %	6.598 m	1.86 cm	
20 %	6.610 m 1.50 cm		
50%	6.605 m	1.14 cm	

Table 1. Mean of observed heights and standard deviation of points on each reflectance plate

The reflectance of the target affects greatly on deviation of altitude of the data points. Therefore, the topographic accuracy is expected to be significantly better on surfaces with moderate to high reflectance values.

### 3.2 Spatial Resolution

The spatial resolution of the scanner can be estimated from the collected data sets. At Sjökulla there are wooden frames between areas with different types of pebbles. The wooden frames are 2-4 cm higher than the ground and 2.5 cm wide. When flight altitude was 20 m, the frames are clearly identified in point cloud data (Figure 4). When looking at cross sections, it can be observed that the corners are somewhat rounded, but the frames have an even top surface. This indicates that from an altitude of 20 m the spatial resolution of the scanner is better than 2.5 cm. From an altitude of 50 m the frames are barely visible, but as they are still distinguishable it indicates that the scanner can pick up features of roughly that size. From the altitude of 100 m the frames are not distinguishable, but also the point density has already become quite sparse so it is difficult to say whether flying slower would have made the features visible.

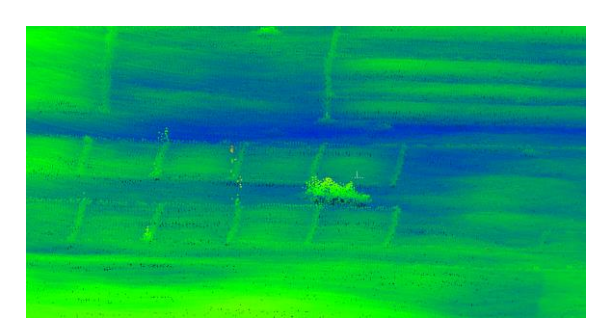


Figure 4. Point cloud data of Sjökulla from altitude of 20 m. Colouring of points is based on the z-coordinate.

### 3.3 Depth Performance

The bathymetric performance was determined using data collected from Lake Vitträsk. On the first day, when weather

conditions were excellent, one flight was flown at an altitude of 20 m. In the point cloud collected on this flight, the lake bottom was visible up to depth of 4.2 meters. A cross section of this point cloud is visible in Figure 5. This result is unexpected as the Secchi depth at Lake Vitträsk was estimated to be only 2.4 m and as is expressed in Section 2.1, Fraunhofer IPM has specified the penetration depth to be one Secchi.



Figure 5. Cross section of the point cloud of first day's flight at Lake Vitträsk. Lake bottom was visible up to depth of 4.2 m.

Having a penetration depth of nearly twice the advertised value is quite exceptional even if the weather conditions were good as generally manufacturers tend to announce the performance of their device in favourable conditions as well. Additionally, during the measurements the pulse frequency of the ABS was 50kHz instead of 35kHz as is manufacturer-specified together with the penetration depth of one Secchi. So better depth performance is not explained by using longer pulses. The depth penetration of 1.75 SD can be considered impressive for a lightweight system since many much larger systems advertise to perform similarly (RIEGL a and b; Guo et al., 2022).

On the second day weather conditions were quite challenging so the penetration depth is not expected to be as good as on the first day. A total of four flights were flown from different altitudes on this day and the submerged metal sheets were used as reference targets. As can be seen in Figure 6 the plates at depths of 2 and 3 meters are visible from all altitudes, but the ones positioned deeper are not visible in any of the data sets. Figure 6 shows cross sections of the 3D point clouds constructed from the data collected with the sensor from specified flight altitudes. The three meter plate consist of fewer points as the altitude increases, but even from 80 meters it is clearly visible and, for example, fitting a plane based on the points is possible.

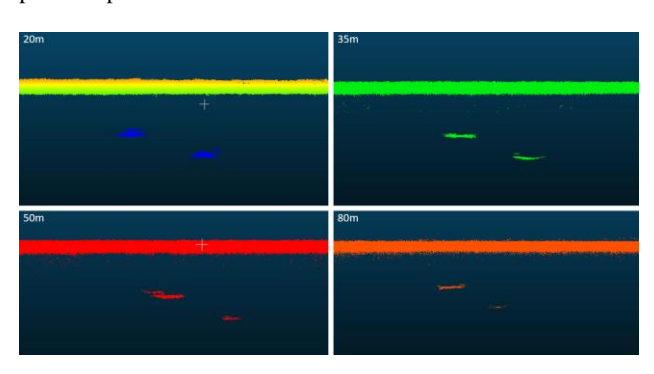


Figure 6. Point clouds of the reference plates at the depths of 2 m and 3 m from different flight altitudes 20, 35, 50 and 80 m.

Thus, the scanner has a penetration depth of over one Secchi depth even in difficult conditions and also from altitude higher than the intended maximum altitude of 50 meters. In more challenging weather conditions, the lake bottom was visible from 20 m altitude up to 2.6 meters, which slightly decreases as altitude increases, until from altitude of 80 m the bottom is visible up to 2.3 meters. The difference is 30 cm and similar to what can be assumed from the reference plates. Based on the

results, altitude clearly has much smaller effect on the performance compared to weather conditions, which might be beneficial as flying higher allows to survey wider area in one go. But on the other hand, it is usually not that much more work to fly some extra lines compared to having to do another field campaign due to prevailing weather conditions.

As the results indicate, the ABS outperforms the advertised bathymetric performance in challenging weather as well as from higher altitudes than originally intended. The slight differences in penetration depth from all examined altitudes further highlight the challenges of bathymetric LiDAR, as it is seen how effortlessly laser travels through air compared to water: Adding tens of meters of air between the scanner and the target only corresponds to decimetre scale changes in the observable water depth.

### 3.4 Bathymetric Accuracy

In addition to the depth penetration, also the accuracy of the bathymetric measurements is an essential factor. This was assessed by comparing detected depth of the submerged reference targets to the actual depth. The obtained results are presented in Table 2. Because the targets at depths of 4 and 5 meters are not visible in the data from any altitudes, those are excluded from the results. In the table the relative depth is expressed in Secchi depths. The depths are measured from the average z-coordinate of data points associated with each target.

Flight	Relative	Actual	Detected	Standard
altitude	depth	depth [m]	depth	deviation
[m]	[SD]		[m]	σ [cm]
20	0.83	$2.00 \pm 0.05$	2.25	9.75
20	1.25	$3.00 \pm 0.05$	3.27	11.8
35	0.83	2.00 ±0.05	2.29	4.51
35	1.25	3.00 ±0.05	3.25	6.50
50	0.83	$2.00 \pm 0.05$	2.46	9.74
50	1.25	3.00 ±0.05	3.56	6.01
80	0.83	$2.00 \pm 0.05$	2.43	7.93
80	1.25	$3.00 \pm 0.05$	3.38	8.29

Table 2. Mean of observed heights and standard deviation of points on each reflectance plate

The standard deviation for bathymetric targets is naturally much higher than for topographic targets. Additionally, there is significantly large variation in the  $\sigma$  values, and neither flight altitude nor depth of the target seem to systematically effect on the values. For each target the detected depth is approximately 30-50 cm larger than the actual depth, which indicates that the refraction correction likely doesn't fully compensate for the distortion caused by refraction. This systematically causes the submerged targets to appear deeper than they actually are. Such behaviour is problematic for surveying water environments as precise data is needed in order to create accurate models. However, possible issues in data processing can be likely fixed with updates to the processing software and known systematic deviations can be compensated in data processing. Therefore, the corrected detected depths describe the performance of the sensor itself better. The detected depths are on average 36.1 cm larger than the actual depths. By correcting the values based on this information, it is seen that the depth differences range from less than two cm to less than twenty, but being generally under ten cm. When the probable systematic deviation is taken into account, the root mean square error is 10.8 cm. Furthermore, without the systematic error the obtained bathymetric vertical accuracy range is comparable to other bathymetric sensors (Wang et al., 2022; Guo et al., 2022) indicating that the performance of the sensor itself is adequate for the application.

### 4. Discussion

The evaluated topo-bathymetric LiDAR scanner, the ABS, demonstrated robust performance in both bathymetric and topographic measurements from UAV platform in this study. Due to its compact size and small weight of approximately 4 kg, the device is well suited for integration on UAV platforms. During the experiments the continuous flight times weren't especially long, but on each day the battery of the drone was changed only once. This further emphasises the importance of lightness of the sensor as it enables rather long flight times with a commercially available drones. This is especially important considering the aim of surveying larger areas, such as river systems. The use of UAV-borne system, such as the ABS, considerably lowers costs compared to conventional multiwavelength ALB with a manned aircraft. Additionally, due to lower flight altitude and more agile manoeuvring it is possible to collect denser LiDAR data and it is easier to avoid occlusions. Another notable benefit of the sensor design is the identical measurement geometry for both green and NIR wavelengths, which eliminates possible errors caused by the differing measurement geometry.

The measurement noise on topographic targets was somewhat higher than expected with standard deviation being 1.5 cm over all four reflectance plates at Sjökulla test field. The results for vertical topographic precision are not as good as with the best topographic LiDAR sensors, but as stated earlier, part of the deviation is caused by the inconsistency on the darkest reflectance plate. The reasons for this remain unclear and perhaps improvements could be pursued through further development or software updates in the future. If only one reflectance plate is examined at a time the vertical precision is on average approximately ±2 cm, which is already in line with typical vertical precision of UAV-borne LiDAR systems (Elaksher et al., 2023; Syetiawan et al., 2020). Good precision is important when considering the applications of bathymetric LiDAR, as for example in flat areas the height difference of a few cm may determine if certain areas are flooded or not Mandlburger et al., 2020; Alho et al., 2009). The precision affects also on the quality of bathymetric data, because well determined water surface is needed for accurate refraction correction. Green laser doesn't only reflect from the surface and bottom, but backscatters from the whole water column causing often a blurry water surface, which is why the multiwavelength capability is important for bathymetric applications as NIR laser does not penetrate the water surface. Further research is needed for more accurate modelling of the true incidence angle determination on water surface, especially on wavy conditions.

The spatial resolution of the sensor is limited by the size of the laser footprint on target. In the collected datasets 2.5 cm wide objects are clearly distinguishable indicating spatial resolution of at least 2.5 cm. As is expected, the resolution decreases as flight altitude, and thus distance to the target, increases. The resolution however remains better than advertised for the whole range of instructed flight altitudes. The high spatial resolution is beneficial for studying water systems and their evolution, as high resolution multiwavelength LiDAR data makes it possible to classify for example the roughness and composition of sediment and type of vegetation both underwater and on the

shore (Tulldahl and Wikström, 2012). The spatial resolution is not precise enough for determining the roughness of fine materials, such as sand or gravel, but it is nevertheless adequate for providing valuable data for fluvial studies.

The penetration depth of the device is almost two Secchi depths during good conditions when the lake surface is calm and there is not direct sunlight causing noise to the sensor. Nearly twice as good result as Fraunhofer IPM states is surprising despite the nearly ideal conditions. As discussed in Section 3.3, this is an excellent result for an UAV-borne lightweight sensor with 50 kHz pulse frequency. During challenging weather conditions the penetration depth was better than one Secchi depth, which still is an outstanding result. The sensor matches the expected performance in all weather conditions where a regular drone can be safely operated. The penetration depth slightly decreases when the flight altitude increases, but the sensor matches the expected performance even from the flight altitude of 80 meters. Higher altitude naturally corresponds to wider survey area, but for very large areas like coastal regions traditional ALB from manned aircraft is likely still more suitable method due to much higher flight speed and wider scanning pattern.

The bathymetric accuracy of the ABS was assessed by comparing the detected depths of submerged reference targets to their actual depths. The results indicate a systematic deviation, with all detected depths averaging approximately 36 cm deeper than the actual depths. This suggests that the refraction correction used in data processing did not fully compensate for the distortions caused at the air-water interface. Part of the difference might be caused simply by the refraction coefficient in the software differing from the real value, since parameters such as salinity or temperature of water are not adjustable. However, as this article studies the performance of the sensor instead of the processing software it is appropriate to assess the bathymetric accuracy also without the probable systematic error. After compensating for the likely systematic error, the ABS performed adequately for a lightweight UAV-borne system, with a root mean square error (RMSE) of about 0.11 m for the perceived depths.

The device performs particularly well in the bathymetric applications, surpassing manufacturer-stated performance. Along with appropriate topographic performance this demonstrates the suitability of the ABS for mapping shallow water environments. Furthermore, the sensor collects the full waveform of received laser pulse that allows more sophisticated waveform processing (Kogut and Bakula, 2019; Allouis et al., 2010). This is often not possible for large ALB systems operated with manned aircraft, because of the much larger size of the study area and thus much larger data amount. The obtained results likely benefit form usage of full waveform data, but as the functioning of the data processing software developed by Fraunhofer IPM is not published this conclusion remains at speculative level.

Deepest reference plates (at 4 and 5 m) were not visible from any altitude despite the sensor being able to see the lake bottom up to the depth of 4.2 meters on the first day. This is unanticipated, because despite the challenging weather the light grey plates were considered to be much easier targets than the lake bottom. However, considering the results from the second day it seems that the difference between the plates and the lake bottom is smaller than was expected. One plausible reason for this is that the lake bottom has less vegetation among the sand

and gravel deeper in the lake, making it appear lighter in colour than at the near shoreline.

The methodology of this study, involving flights at varying altitudes and different days under different conditions, enhances the generality of the findings. Comparisons to both earlier publications and data sheets of larger LiDAR systems suggest that the ABS performs competitively, offering comparable performance in all conditions. However, instead of general performance review, this study is focused especially on the aspects deemed substantial for surveying fresh water environments in Finland, which could limit the applicability of the results in highly differing water environments.

### 5. Conclusions

In this paper the performance of a novel multiwavelength LiDAR sensor, the ABS, is presented and assessed in order to determine its suitability for shallow water bathymetric mapping in freshwater environments and multispectral LiDAR data acquisition in dry land areas using a UAV platform. The lightweight sensor can be mounted on commercially available UAVs reducing operating costs and demonstrates to be a promising tool mapping fresh water environments. The sensor features green and NIR wavelengths with identical measurement geometry, 50 kHz pulse frequency, ToF ranging and is capable of recording full wavelength LiDAR data.

To evaluate the performance and suitability of the system, test flights were conducted at Lake Vitträsk and Sjökulla test field in Finland during 12th and 22nd of October 2023. Assessments of the precision and spatial resolution from topographic targets provide standard deviation of approximately 1.5 cm and spatial resolution is at least 2.5 cm. Despite inconsistencies on the target with low reflectance, the results confirm that the topographic performance is comparable to similar devices and suitable for operation. The bathymetric capabilities of the sensor exceed expectations providing depth penetration of 1.75 Secchi depths in ideal conditions as well as 1.25 Secchi depths in challenging conditions from all altitudes. The depth penetration is comparable to large traditional ALB sensors and can be considered an excellent result for a lightweight UAV-borne sensor. The bathymetric accuracy appears to suffer from systematic deviation caused most probably by insufficient refraction correction in data processing, but by acknowledging this the accuracy of the sensor is at suitable level.

The experimental results demonstrate the topographic and bathymetric performance of the ABS and confirm that the device is suitable to be used for mapping fresh water environments in Finland. Though some inconsistencies in topographic measurements as well as in refraction correction highlight areas for improvement, the sensor's performance on all evaluated aspects meets or exceeds that of established systems used in similar applications. Future research should focus on deploying the ABS in actual study areas to further validate its performance in concrete fluvial environment modelling scenarios.

### Acknowledgements

Authors wish to thank Paula Litkey and Eero Ahokas for their valuable assistance in the implementation of the field tests related to bathymetry. This research was funded by Research Council of Finland and NextGenerationEU through projects Hydro-RI Platform (decision number 346162) and Green-Digi-

Basin (decision number 347702), by Research Council of Finland Flagship project Digital Waters (decision number 359249), and by European Regional Development Fund through project UOMARI (grant number A80681).

### References

Alho, P., Hyyppä H., Hyyppä J., 2009: Consequence of dtm precision for flood hazard mapping. A case study in sw Finland. *Nordic Journal of Surveying and Real Estate Research*, 6, 21–39

Allouis, T., Bailly, J.S., Pastol, Y., Le Roux, C., 2010: Comparison of LiDAR waveform processing methods for very shallow water bathymetry using Raman, near-infrared and green signals. *Earth Surf. Process. Landforms*, 35, 640–650. https://doi.org/10.1002/esp.1959

Beck, H., Zimmermann, N., McVicar, T, Vergopolan, N., Berg, A., Wood, E., 2018: Present and future Köppen-Geiger climate classification maps at 1-km resolution. *Scientific data*, 5, 180214. https://doi.org/10.1038/sdata.2018.214

Elaksher, A., Ali, T., Alharthy, A., 2023: A Quantitative Assessment of LIDAR Data Accuracy. *Remote Sens*, 15, 442. https://doi.org/10.3390/rs15020442

Fernandez-Diaz, J.C., Glennie, C.L., Carter, W.E., Shrestha, R.L., Sartori, M.P., Singhania, A., Legleiter, C.J., Overstreet, B.T., 2014: Early results of simultaneous terrain and shallow water bathymetry mapping using a single-wavelength airborne LiDAR sensor. *IEEE J. Sel. Top. Appl. Earth Observ. Remote Sens.*, 7, 623–635. https://doi.org/10.1109/JSTARS.2013.2265255

Fraunhofer IPM a. Airborne Bathymetric Laser Scanner Datasheet. 2023. Fraunhofer Institute for Physical Measurement Techniques, Georges-Köhler-Allee 301, 79110 Freiburg, Germany. Available online: https://www.ipm.fraunhofer.de/en (Accessed on 15.10.2023).

Fraunhofer IPM b, TECHNICAL SPECIFICATIONS AIRBORNE BATHYMETRIC SCANNER ABS, Fraunhofer Institute for Physical Measurement Techniques: Georges-Köhler-Allee 301, 79110 Freiburg, Germany, 2023.

Girardeau-Montaut, D., 2015: CloudCompare: 3D point cloud and mesh processing software. Open Source Project, 197

Guenther, G.C., Cunningham, A.G., Laroque, P.E., Reid, D.J., 2000: Meeting the Accuracy Challenge in AirborneLidar Bathymetry. In *Proceedings of the 20th EARSeL Symposium: Workshop on Lidar Remote Sensing of Land and Sea*, Dresden, Germany, 16–17 June 2000

Guo, K., Li, Q., Wang, C., Mao, Q., Liu, Y., Zhu, J., Wu, A., 2022: Development of a single-wavelength airborne bathymetric LiDAR: System design and data processing. *ISPRS J. Photogramm. Remote Sens.*, 185, 62–84. https://doi.org/10.1016/j.isprsjprs.2022.01.011

Heino, J., Culp, J.M., Erkinaro J., Goedkoop W., Lento J., Rühland K.M., Smol J.P., 2020: Abruptly and irreversibly changing Arctic freshwaters urgently require standardized monitoring. *Journal of Applied Ecology*, 57, 1192–1198. https://doi.org/10.1111/13 65-2664.13645

- Hirabayashi, Y., Mahendran, R., Koirala, S., Konoshima L., Yamazaki D., Watanabe S., Kim H., Kanae S., 2013: Global flood risk under climate change. *Nature Clim Change*, 3, 816–821. https://doi.org/10.1038/nclimate1911
- Idris, M.S., Siang, H.L., Amin, R.M., Sidik, M.J., 2022: Two-decade dynamics of MODIS-derived Secchi depth in Peninsula Malaysia waters. *Journal of Marine Systems*, 236, 103799. https://doi.org/10.1016/j.jmarsys.2022.103799
- Islam M.T., Yoshida K., Nishiyama S., Sakai K., Tsuda T., 2020: Characterizing vegetated rivers using novel unmanned aerial vehicle-borne topo-bathymetric green lidar: Seasonal applications and challenges. *River Research and Applications*, 38(1), 44–58. https://doi.org/10.1002/rra.3875
- Kasvi, E., Salmela, J., Lotsari, E., Kumpula, T., Lane, S.N., 2019: Comparison of remote sensing based approaches for mapping bathymetry of shallow, clear water rivers. *Geomorphology*, 333, 180–197. https://doi.org/10.1016/j.geomorph.2019.02.017
- Kogut, T., Bakuła, K., 2019: Improvement of FullWaveform Airborne Laser Bathymetry Data Processing based on Waves of Neighborhood Points. *Remote Sens.*, 11, 1255. https://doi.org/10.3390/rs11101255
- Leica. Chiroptera-5 product specifications. 2022. Leica Geosystems AG, Heinrich-Wild-Strasse, CH-9435 Heerbrugg, Switzerland. Available online: https://www.leica-geosystems.com (Accessed on 07.10.2024).
- Li, X., Yang, B., Xie, X., Li, D., Xu, L., 2018: Influence of Waveform Characteristics on LiDAR Ranging Accuracy and Precision. *Sensors*, 18, 1156. https://doi.org/10.3390/s18041156
- Mandlburger, G., Pfennigbauer, M., Schwarz, R., Flöry S., Nussbaumer, L., 2020: Concept and Performance Evaluation of a Novel UAV-Borne Topo-Bathymetric LiDAR Sensor. *Remote sensing*, 12, 986. https://doi.org/10.3390/rs12060986
- Okhrimenko, M., Hopkinson, C., 2019: A simplified end-user approach to lidar very shallow water bathymetric correction. *IEEE Geosci. Remote Sens. Lett.*, 17, 3–7. http://doi.org/10.1109/LGRS.2019.2915267
- Pfennigbauer M., Ullrich A., 2011: Multi-wavelength Airborne Laser Scanning. International LIDAR Mapping Forum, New Orleans, 7-9 February 2011
- RIEGL a. VQ-880-G II Data Sheet. 2022. RIEGL Laser Measurement Systems GmbH, Riedenburgstraße 48, 3580 Horn, Austria. Available online: http://www.riegl.com (Accessed on 07.10.2024).
- RIEGL b. VQ-880-GH Data Sheet. 2022. RIEGL Laser Measurement Systems GmbH, Riedenburgstraße 48, 3580 Horn, Austria. Available online: http://www.riegl.com (Accessed on 07.10.2024).
- Syetiawan, A., Gularso, H., Kusnadi, G.I., Pramudita, G.N., 2020: Precise topographic mapping using direct georeferencing in UAV. *IOP Conf. Ser.: Earth Environ. Sci.*, 500, 012029. https://doi.org/10.1088/1755-1315/500/1/012029

- Tulldahl, H.M., Wikström, S.A., 2012: Classification of aquatic macrovegetation and substrates with airborne lidar. *Remote Sensing of Environment*, 121, 347–357. https://doi.org/10.1016/j.rse.2012.02.004
- U.S. Marine Corps, STANDARD OPERATING PROCEDURES FOR LASER HAZARDS CONTROL, United States Marine Corps Air Ground Combat Center: 1502 5th St Twentynine Palms, CA, USA, 2014
- Vosselman, G., Maas, H.-G., 2010. Airborne and Terrestrial Laser Scanning, Whittles Publishing: Dunbeath, Scotland, UK, pp. 21–39.
- Walkera. R1000 RTK A new look Industry Drone. 2022. Walkera Technology Co. Ltd., Taishi Industrial Park, Dongchong, Nansha Dist, Guangzhou, China. Available online: https://en.walkera.com/index.php?id=r1000 (Accessed on 27.08.2024).
- Wang, D., Xing, S., He, Y., Yu, J., Xu, Q., Li, P., 2022: Evaluation of a New Lightweight UAV-Borne Topo-Bathymetric LiDAR for Shallow Water Bathymetry and Object Detection. Sensors, 22, 1379. https://doi.org/10.3390/s22041379
- Werner, C. S., Gangelhoff, J., Frey, S., Steiger, D., Reiterer, A., 2023: Development of a compact pulsed time-of-flight LiDAR platform for underwater measurements. *The International Hydrographic Review*, 29(2), 200–207. https://doi.org/10.58440/ihr-29-2-n09
- Westfeld, P., Maas, H.G., Richter, K., Weiß, R., 2017: Analysis and correction of ocean wave pattern induced systematic coordinate errors in airborne LiDAR bathymetry. *ISPRS J. Photogramm. Remote Sens.*, 128, 314–325. https://doi.org/10.1016/j.isprsjprs.2017.04.008
- Young A.P., Ashford S.A., 2006: Application of Airborne LIDAR for Seacliff Volumetric Change and Beach-Sediment Budget Contributions. *Journal of Coastal Research*, 22, 307–318. http://dx.doi.org/10.2112/05-0548.1